7.34-μs Continuously Tunable Parametric Delay

Yitang Dai,[1] Yoshitomo Okawachi,[1] Amy Turner-Foster,[2] Michal Lipson,[2] Alexander Gaeta,[1] and Chris Xu[1]

[1]*School of Applied and Engineering Physics, Cornell University, Ithaca, NY 14853*
[2]*School of Electrical and Computer Engineering, Cornell University, Ithaca, NY 14853*
yd82@cornell.edu

Abstract: A wavelength-transparent, continuously-tunable 7.34-μs all-optical delay is demonstrated for 10-Gb/s NRZ signal by cascading discrete and continuous stages. 3.7- to 4.3-dB penalty is reported for the entire system that includes four successive silicon-based parametric processes.

OCIS codes: (060. 2330) Fiber optics communications; (190.4380) Nonlinear optics, four-wave mixing.

1. Introduction

The ability to create precise all-optical delays, i.e., being able to control the arrival times of optical data streams on the physical level, is highly desirable in many areas such as communication networking [1], optical control of phased array antennas [2], optical sampling [3], and others. Discrete optical delays, generated by combining a series of fixed delay lines with different amounts of delay in parallel [4], are capable of a large range of tunable delays. However, continuously tuning is required as the data rate increases. Large continuously tunable delays are usually achieved by the "wavelength conversion and dispersion" delay scheme, which takes advantage of wavelength conversion from four-wavelength mixing (FWM) in silicon waveguides or highly nonlinear fiber (HNLF) and the group-velocity dispersion (GVD) in an optical fiber for generating a wavelength-dependent optical delay [5-15]. The total delay is approximately the product of the GVD parameter, the length of the dispersive fiber, and the wavelength shift. As a result, large ranges of delay can be obtained by simply extending the fiber length or the wavelength conversion bandwidth, and delay ranges larger than 1 μs have been demonstrated experimentally [12, 13].

There are several limitations in extending the fiber length to increase the delay range. The accumulated residual dispersion slope and polarization mode dispersion will impact the system performance, particularly at high data rates [12]. Furthermore, the significant fiber loss needs to be compensated by optical amplifications, which degrades the system optical signal-to-noise ratio (OSNR) and increases the delay line power consumption. Note that 60 km of dispersion compensation fibers (DCFs) or more were used to achieve a 1-μs delay range [12, 13]. In comparison, a fixed 1-μs delay can be generated by a standard single-mode fiber (SSMF) of 200 meters in length with negligible impact to the data fidelity, even at data rates of 100 Gb/s. Thus, the combination of discrete and continuously tunable delays can be an effective approach to achieve simultaneously fine, continuous tuning and an ultra-large delay range. In this paper, we report the first continuously tunable optical delay line with extended delay range via a cascading discrete stage. A 7.34-μs continuous tuning range is achieved using a discrete stage with 16 wavelength-dependent delays and a continuously tunable stage capable of 711-ns delay range. Using the wavelength-optimized optical phase conjugation scheme [12], zero residual GVD is achieved throughout the tuning range. The bit-error-rate (BER) performance of the system is experimentally characterized using 10-Gb/s NRZ data.

2. Experiment

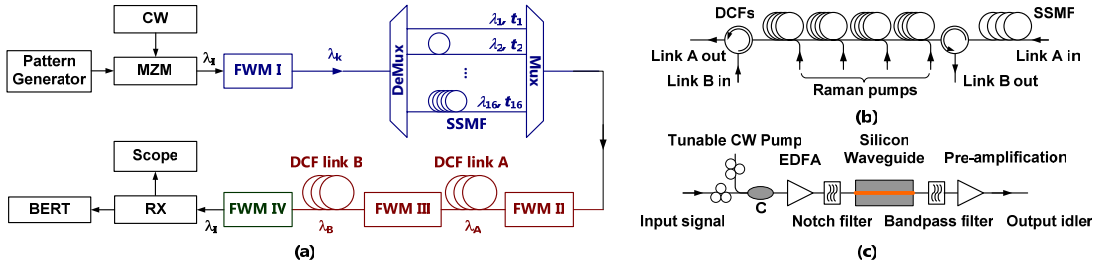

Fig. 1. (a) The experimental setup. (b) The setup for the two DCF links. Raman pumps are used in each DCF spools to compensate for the 40-dB loss in the link throughout the tuning range. (c) The setup for each of the four wavelength conversion stages utilizing silicon waveguides.

The experimental setup is illustrated in Fig. 1(a). A CW DFB laser centered at λ_1 = 1563.5 nm is modulated using an MZM, generating the NRZ data as the input signal of the tunable delay system. The discrete stage, consisting of a pair of 200-GHz, 16-channel Mux / DeMux and 16 SSMFs with suitable lengths between them, provides a discrete tunable delay with very large granularity of hundreds of nanoseconds when its input wavelength is tuned among the 16 wavelengths by the first wavelength conversion. The length of the SSMFs in each discrete channel is measured by an oscilloscope at approximately 1-ns precision. The discrete delay stage is followed by a

continuous tuning stage, containing the following two wavelength conversion elements and two DCF links, which provides a continuous tuning that is slightly larger than any of the delay steps between the adjacent discrete channels. As a result, a continuously tunable delay is achieved without any gaps, and the delay range of the continuous tuning is multiplied. As shown in Fig. 1 (b), four 15-km spools of DCF with a dispersion parameter of ~ -250 ps/nm/km are used as the two DCF links by using two circulators. A 4-km SSMF spool is used before the first circulator to shift the dispersion curve of link A by ~ 65 ps/nm. A fourth wavelength conversion ensures the wavelength preserving operation. The system output is detected by a standard 10-Gb/s receiver and evaluated by an oscilloscope and a BER tester (BERT). The four silicon-based FWM setups, shown in Fig. 1(c), are the same as those described in [12, 14].

Tunable delays are obtained by tuning λ_k, λ_A, and λ_B, the wavelengths in the discrete stage, link A, and link B, respectively. k is the channel number. Note that the dispersion in the DCFs that generates the wavelength-dependent delay also distorts the signal, and the phase distortion introduced by the SSMFs of the discrete stage can be significant for transmissions at high data rate. In order to support high data rate transmissions, our system is designed to achieve zero GVD at the final output throughout the delay tuning range. The residual GVD of the continuous stage, based on the wavelength-optimized phase conjugating process [12], is used to compensate that of the discrete stage [see Fig. 2(a)]. λ_B is now determined by λ_k (discrete tuning) and λ_A (continuous tuning):

$$\chi_A(\lambda_A) - \chi_B(\lambda_B) = \chi_k \tag{1}$$

where χ_k is the dispersion of kth channel of the discrete stage, and $\chi_A(\lambda)$ and $\chi_B(\lambda)$ are the dispersion function for DCF links A and B, respectively. In our system, the requirement for a zero residual dispersion [Eq. (1)] results in a 1- to 4-nm blue shift of λ_B from λ_A.

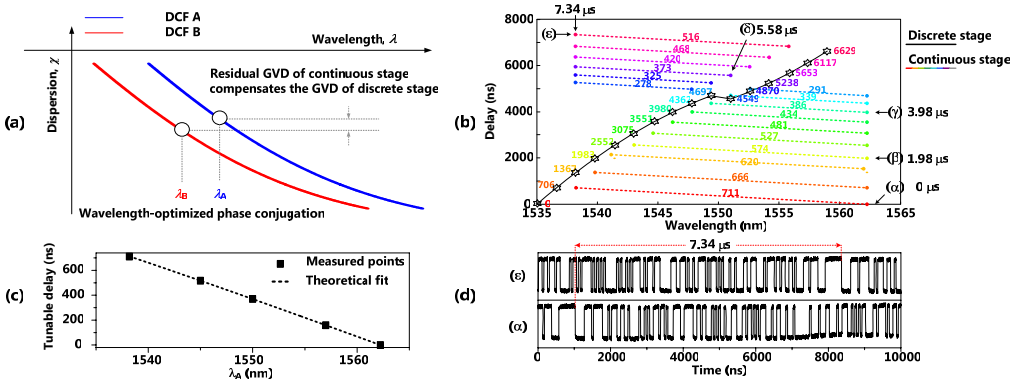

Fig. 2. (a) Dispersion management scheme to achieve zero residual GVD for the entire delay system. (b) The tunable delay values in terms of the discrete (λ_k, black line) and the continuous (λ_A, colored lines) wavelength tunings. ✡ points indicate the positions for the 16 discrete channels: the wavelengths and the delay values. The colored lines show the wavelength tuning and the delay range of the continuous stage when the corresponding discrete delay is chosen. (c) Measured tunable delay of the continuous stage as a function of λ_A when the 1st channel is chosen. The delay is measured directly by an oscilloscope with a data pattern at 100 Mb/s. (d) The measured 7.34-μs delay between the shortest delay setting at (α) and the longest delay setting at (ε). A data pattern at 20 Mb/s is used for the measurement.

We performed both the discrete and the continuous wavelength tuning within the C-band of the EDFA, taking advantage of the mature and low-cost optical devices (e.g. filters and amplifiers) within this band. The wavelength conversion ranges of the two stages overlap since 16 200-GHz channels cover a large portion of the C-band. Due to the requirement to spectrally separate the idler from the signal and the pump in each of the FWM stages, there should be a minimum wavelength separation between the signal and the idler. As a result, the wavelength λ_k of the kth channel in the discrete stage should not overlap with the wavelength tuning range of the continuous stage when the kth channel is used. Otherwise there would be a gap in the tunable delay since λ_A cannot be tuned continuously in the vicinity of λ_k. In our design, we confine the tuning range of λ_A within either the blue side or the red side of λ_k, depending on which side provides a larger continuously tunable delay range. The wavelength ranges used in the experiment are shown in Fig. 2(b) (colored lines). By compromising the maximum delay range, we achieve both the discrete and the continuous tuning within the C-band.

The total delay of the entire system is simply the sum of the discrete and the continuous parts, see the first line of Eq. (2). According to [12] the delay in the continuous stage can be expressed in terms of the wavelengths λ_A and λ_B, and the dispersion functions $\chi_A(\lambda)$ and $\chi_B(\lambda)$ for DCF links A and B, respectively. The delay in the discrete stage, τ_{discrete}, is determined by the fiber length in each channel. The total delay of the system is then

$$\begin{aligned}\tau(k,\lambda_A,\lambda_B) &= \tau_{\text{discrete}}(k) + \left[\int_{\lambda_{A,1}}^{\lambda_A}\chi_A(\lambda)d\lambda + \int_{\lambda_{B,1}}^{\lambda_B}\chi_B(\lambda)d\lambda\right] \\ &= \tau_{\text{discrete}}(k) + \left[\int_{\lambda_{A,1}}^{\lambda_{A,k}}\chi_A(\lambda)d\lambda + \int_{\lambda_{B,1}}^{\lambda_{B,k}}\chi_B(\lambda)d\lambda\right] + \left[\int_{\lambda_{A,k}}^{\lambda_A}\chi_A(\lambda)d\lambda + \int_{\lambda_{B,k}}^{\lambda_B}\chi_B(\lambda)d\lambda\right]\end{aligned} \tag{2}$$

where $\lambda_{A,k}$ and $\lambda_{B,k}$ are the starting points (longest wavelengths) of the wavelength conversion ranges in DCF links A and B, respectively, when the kth channel is used. $\lambda_{A,1}$ and $\lambda_{B,1}$ are the reference wavelengths, i.e., $\tau(k=1, \lambda_A=\lambda_{A,1}, \lambda_B=\lambda_{B,1})=0$. The delay can also be expressed explicitly in terms of the starting wavelengths in the DCF links when the kth discrete channel is selected. This is shown in the second line of Eq. (2). The values of the continuous delay tuning within each discrete channel (represented by the third term in the second line of Eq. (2) [12]) are measured and indicated in Fig. 2(b) (the values above the colored lines). In particular, the measured tunable delay for the 1st channel, which has the largest wavelength tuning range, as a function of λ_A is plotted in Fig. 2(c), showing a total delay range of 711 ns. The step of the discrete delay [the first two terms in the second line of Eq. (2)] is designed to be 4 to 5 ns less than the corresponding continuous tuning range, ensuring continuous tuning between two adjacent discrete channels. For the entire system, the delay values at five points, as shown from (α) to (ε) [see labels in Fig. 3(a)], are measured. As shown in Fig. 2(d), the combined discrete and continuous stages provide a tunable delay from 0 to 7.34 μs. The 7.34-μs delay range is significantly larger than previous experiments that use continuous stage only [12, 13].

It is interesting to note that the discrete delays include two contributions: (1) the discrete delay introduced by the SSMF [$\tau_{discrete}$, the first term in second line of Eq. (2)], and (2) a channel offset due to the variations in the starting wavelengths of the continuous stage (the second term). Since the last 6 discrete channels have starting points other than $\lambda_{A,1}$, the channel offsets are nonzero for $k > 10$. As shown in Fig. 2(b), these channel offsets were taken into account by shortening the SSMFs accordingly for delay channels 11 through 16.

We measured the BER performance of the entire system after four parametric processes using a 10 Gb/s NRZ data channel with a 2^{31}-1 PRBS sequence. Five delay points from (α) to (ε) are measured. Figure 3(a) shows the optical spectra of the four silicon-based FWMs when the γ point is measured. Although the wavelength conversion efficiency in current silicon waveguides is not high, at approximately -20 dB on-off conversion efficiencies in our experiment, good OSNRs of the idler waves can be achieved after the FWM process by using notch filters before the Si-waveguides, which eliminate the ASE noise at the spectral regions where the idlers will be generated [12]. Figure 3(b) shows the BERT results of the five measured points after the whole system with four cascading wavelength conversion stages. The measured power penalty is 3.7 to 4.3 dB at a BER of 10^{-9}. Our experiment demonstrates that all four wavelength conversion processes can be accomplished using the Si nanowaveguides.

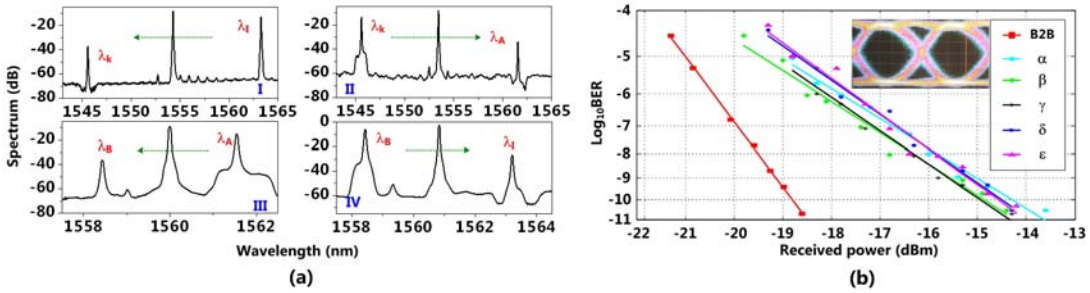

Fig. 3. (a) Optical spectra of the four FWMs for achieving the delay value at the γ point. Arrows show the wavelength conversion directions. (b) Measured BER curves of back-to-back (B2B) and after transmission through the entire tunable delay systems at different delays. Insert shows the eye-diagram measured at γ delay at a BER of less than 10^{-11}.

3. Conclusion

We demonstrated an all-optical, continuously tunable parametric delay system by cascading the discrete and the continuous tuning stages. A large tuning range of 7.34 μs is achieved. The wavelength-optimized optical phase conjugation scheme was used to minimize the residual dispersion of the system, making the delay system capable of high data rate transmission. Four successive wavelength conversions were performed using silicon waveguides. The system BER performance was measured for 10 Gb/s NRZ data with a power penalty of 3.7 to 4.3 dB.

References

[1]. M. K. Dhodhi, et al, Comput. Commun. **24**, 1726 (2001).
[2]. J. L. Corral, et al, Photon. Technol. Lett. **9**, 1529 (1997).
[3]. Y. Han et al, J. Lightwave Technol. **21**, 3085 (2003).
[4]. S. J. B. Yoo, J. Lightwave Technol. **24**, 4468 (2006).
[5]. J. Van, el tal, Opt. Lett. 30, **99** (2005).
[6]. J. E. Sharping, et al, Opt. Express **13**, 7872 (2005).
[7]. J. Ren, et al, ECOC 2006, Th4.4.3 PDP.
[8]. Y. Wang, et al, Photon. Technol. Lett. **19**, 861 (2007).
[9]. Y. Okawachi, et al, Opt. Express **16**, 10349 (2008).
[10]. E. Myslivets, et al, Photon. Technol. Lett., **21**, 251 (2009).
[11]. L. C. Christen, et al, Opt. Lett. **34**, 542 (2009).
[12]. Y. Dai, et al, Opt. Express, **17**, 7004 (2009).
[13]. E. Myslivets, et al, Opt. Express **17**, 11958 (2009).
[14]. Y. Dai, et al, Opt. Express, Opt. Express, **17**, 16029 (2009).
[15]. S. R. Nuccio, et al, Opt. Lett. **34**, 1903 (2009).